

Distributions of charged particles at 13 TeV with CMS

Juan Manuel Grados Luyando^{*†}

Deutsches Elektronen-Synchrotron (DESY) - Hamburg

E-mail: juan.grados.luyando@desy.de

Pseudorapidity distributions of charged-particles, $dN_{\text{ch}}/d\eta$, produced in proton-proton collisions at a centre-of-mass energy $\sqrt{s} = 13$ TeV are measured in the pseudorapidity range $|\eta| < 2.4$ for charged-particles with a transverse momentum $p_T > 0.5$ GeV [1]. Measurements are presented for four event categories. The first two categories correspond to inclusive and inelastic enhanced event samples. The other two categories are disjoint subsets of the inelastic enhanced event sample that are either enhanced or depleted in single diffractive dissociation events. The measurements are compared to predictions from Monte Carlo event generators which were tuned to describe the underlying event properties at lower centre-of-mass energies.

*XXIV International Workshop on Deep-Inelastic Scattering and Related Subjects
11-15 April, 2016
DESY Hamburg, Germany*

^{*}Speaker.

[†]On behalf of the CMS collaboration.

1. Introduction

In high energy hadron-hadron collisions the majority of the processes are soft, i.e., without any hard scattering of the partonic constituents of the proton. In contrast with the hard scattering events, well described by perturbative quantum chromodynamics (pQCD), such events are generally modelled phenomenologically to describe the elastic scattering, diffractive dissociation and non-diffractive scattering, as well as, multi partonic interaction (MPI) from a soft to a semi-hard scale. These phenomenological models contain free parameters which have to be adjusted with the information of the experimental measurements, so-called tuning.

Inclusive measurements of charged-particle pseudorapidity distributions, $dN_{\text{ch}}/d\eta$, and transverse momentum distributions, $dN_{\text{ch}}/dp_{\text{T}}$, have previously been performed in pp and p $\bar{\text{p}}$ collisions for different centre-of-mass energies and phase space regions [2–16], where η is defined as $-\ln[\tan(\theta/2)]$, with θ being the polar angle of the particle trajectory with respect to the anticlockwise-beam direction. Here, charged-particle pseudorapidity distributions, also referred to as charged-particle pseudorapidity densities, are measured with the CMS detector in pp collisions at a centre-of-mass energy $\sqrt{s} = 13$ TeV for all charged-particles with a transverse momentum $p_{\text{T}} > 0.5$ GeV in the range $|\eta| < 2.4$. The first measurement of the charged hadron pseudorapidity distribution, $dN_{\text{had}}/d\eta$, at $\sqrt{s} = 13$ TeV by CMS is reported in [2].

In this analysis different MC event generators and tunes are used for data corrections and comparisons with the final corrected results. These are PHYTHIA8 [17] with the tunes Monash [18], CUETP8M1 (also referred as CUETM1) [19] and CUETP8S1 (also referred as CUETS1) [19], PHYTHIA8 event generator implementing the MBR [20] model, also referred to as PHYTHIA8 MBR with the tunes 4C [21] and CUETP8M1. HERWIG++ [22] event generator is used with the tune UE-EE-4C [23], and the event generator EPOS [24] with the LHC tune [25, 26] based on EPOS 1.99. These event generators and tunes differ in the treatment of the initial- and final-state radiation, hadronisation, colour reconnections, and cutoff values of the MPI mechanism, as well as the implementation of diffractive events. These tunes were obtained from comparisons with measurements of minimum bias (MB) and underlying event (UE) observables, from Tevatron and LHC experiments.

In this publication only a reduced number of MC event generators are discussed, a more complete discussion can be found in the original publication [1].

2. Event selection and systematic effects

The data are collected with a zero bias trigger in a special run in summer 2015 and have an average value of 1.3 pp interactions per bunch crossing [27], so-called pileup. Beam Pick-up Timing for the eXperiments (BPTX) devices are used to trigger the detector readout. They are located around the beam pipe at a distance of 175 m from the IP on either side, and are designed to provide precise information on the bunch structure and timing of the incoming beams. The zero bias data sample consists of 3.9 million events triggered by the presence of both beams crossing at the IP. The requirement of a primary vertex gives a sample of 1.75 million events.

Rejection of beam background events and events with more than one collision per bunch crossing is achieved by requiring exactly one reconstructed primary vertex. The vertex is required to be

within $|z| < 15$ cm with respect to the position of the beam spot along the beamline. The transverse distance with respect to the beam spot position is required to be smaller than 0.2 cm. A minimal number of 2 tracks is required in the vertex fitting, corresponding to a number of degrees of freedom greater than zero in the vertex fitting procedure.

High-purity tracks [28] are selected with a transverse momentum $p_T > 0.5$ GeV in order to allow a reasonable tracking efficiency, and a relative transverse momentum uncertainty smaller than 10%. Tracks are measured within the pseudorapidity range $|\eta| < 2.4$ corresponding to the fiducial acceptance of the tracker, in order to avoid effects from tracks very close to the geometric edge of the tracking detector. A track-vertex association is applied by requiring impact parameter with respect to the primary vertex position both in the transverse plane and along the z-axis, to be each less than 3. The number of pixel hits associated to a track has to be greater or equal to 3 in the central pseudorapidity region $|\eta| < 1$ and greater or equal to 2 in $|\eta| > 1$.

The event selection based on the HF calorimeters makes use of the HF towers with an energy threshold of 5 GeV in the fiducial acceptance $3 < |\eta| < 5$. The activity in the calorimeters is defined by the presence of at least one tower with an energy above the threshold value. The veto condition is defined otherwise by the absence of towers with an energy above the threshold value. An inelastic-enhanced event sample is defined by requiring the presence of activity in either side of the calorimeters. A NSD-enhanced sample is defined by requiring activity in both sides of the calorimeters. A SD-enhanced sample is defined by requiring activity in exactly one side of the calorimeters, the veto condition being applied to the other side. In addition, an inclusive event sample is defined by only requiring the presence of exactly one primary vertex in the event, without applying the selection based on the HF calorimeters.

The measurements are corrected for the track reconstruction and event-selection efficiencies. The corrected distributions refer to stable primary charged particles, either directly produced in pp collisions or from decays of particles with decay length $c\tau < 1$ cm, where τ is the lifetime of the particle and c the speed of light. On the stable-particle level, events are selected if at least one charged particle is found in $|\eta| < 2.4$ with $p_T > 0.5$ GeV. The activity in the forward region $3 < |\eta| < 5$ is defined by the presence of at least one particle with an energy above 5 GeV. The veto condition is defined otherwise by the absence of particles with an energy above 5 GeV. The inelastic-enhanced event sample is defined by requiring activity in the pseudorapidity range $3 < \eta < 5$ or $-5 < \eta < -3$. The NSD-enhanced sample is defined by requiring activity in the regions $3 < \eta < 5$ and $-5 < \eta < -3$. The SD-enhanced sample is defined by requiring activity in either the positive or negative η range, the veto condition being applied to the other region. The SD-enhanced sample is further divided into two disjoint subsets according to the η region in which the activity is present. In addition, measurements are shown for an inclusive selection, with no requirement on the activity in $3 < |\eta| < 5$, and only the requirement of at least one charged particle with $|\eta| < 2.4$ and $p_T > 0.5$ GeV.

Several sources of systematic uncertainties affect the results. These include model dependence, the difference between the track reconstruction efficiency in data and simulation, event selection and the modelling of the pileup contribution. The systematic uncertainties have been added accounting for the correlations between them. The total systematic uncertainty shows a constant behaviour as a function of η . Their contribution is summarized in Table. 1.

Systematic effect	Inclusive	Inelastic	NSD	SD
Model Dependence	1%	1%	0.5%	7%
Event selection	N.A.	0.1%	0.5%	4%
Pile Up dependence	1.5%	1.5%	3%	4%
Track reconstruction	4%			
Total	4.5%	4.5%	5%	10%

Table 1: Summary of systematic uncertainties for the different event selections.

3. Results

The data points and uncertainties are symmetrized in $\pm\eta$. The measurements are first corrected to the same stable-particle level as the one used in Ref. [2] for the measurement of the pseudorapidity distribution of charged hadrons in pp collisions at $\sqrt{s} = 13$ TeV. The charged-hadron pseudorapidity densities are compared in Fig. 1 and found to be in good agreement.

The charged-particle pseudorapidity density for the inclusive selection at $\sqrt{s} = 13$ TeV is compared in Fig. 2 to previous CMS measurements at lower centre-of-mass energies $\sqrt{s} = 900$ GeV and 7 TeV [29]. The measurements are compared to predictions of various Monte Carlo event generators.

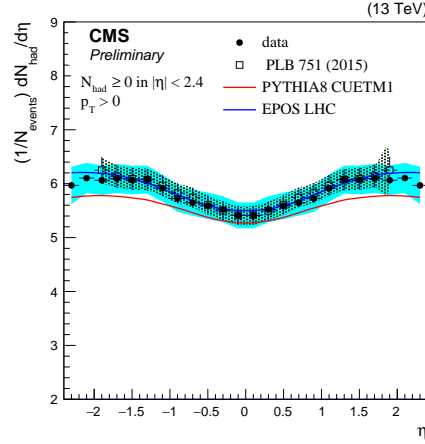


Figure 1: Comparison between the charged-hadron pseudorapidity densities determined in this analysis (full circle) and in Ref. [2] (open square).

Figures 3-4 show the charged-particle pseudorapidity densities for the inclusive, inelastic-enhanced, NSD-enhanced and SD-enhanced selections. The total systematic uncertainties are shown as shaded bands around the data points. The charged-particle pseudorapidity densities are about 3 for the inclusive and inelastic-enhanced selections, slightly higher for the NSD-enhanced sample and about 0.7 for the SD-enhanced selection. The measurements are compared to predictions of various Monte Carlo event generators. The different predictions are in reasonable agreement with the data.

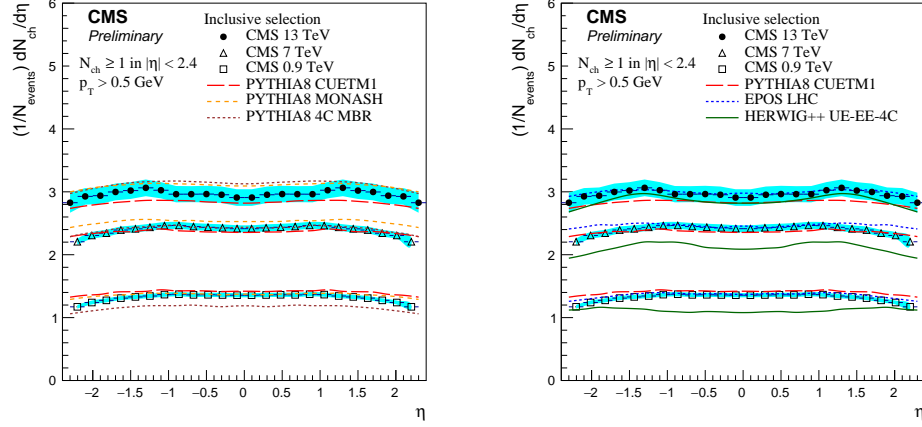


Figure 2: Charged-particle pseudorapidity density for the inclusive event sample measured by CMS at different centre-of-mass energies $\sqrt{s} = 900$ GeV, 7 TeV and 13 TeV. The total systematic uncertainties are shown as shaded bands encompassing the data points.

For the inclusive and inelastic-enhanced samples, the predictions of PHYTHIA8 with the tune CUETS1 and PHYTHIA8 MBR with the tune CUETM1 give the best description of the data.

For the NSD-enhanced sample, the predictions of PHYTHIA8 with the tune CUETM1 and PHYTHIA8 MBR with the tune CUETM1 give the best description of the data, while PHYTHIA8 MBR with the tune 4C overestimate the measurements.

For the SD-enhanced samples, the predictions of PHYTHIA8 MBR with the tune 4C describe the data well. The predictions of PHYTHIA8 with the tunes CUETM1 and CUETS1, and PHYTHIA8 MBR with the tune CUETM1 overestimate the measurements. All the predictions shown here are able to describe the charged-particle pseudorapidity density on the η side associated to the direction of the diffractively scattered proton. The only predictions which are able to describe the activity on the η side of the diffractively produced final state are those of PHYTHIA8 MBR with the tune 4C.

4. Conclusions

The charged-particle pseudorapidity density in four different event categories have been presented at a centre-of-mass energy of $\sqrt{s} = 13$ TeV for the first time. The measurements are compared to various MC event generators predictions implementing different approaches for the initial- and final-state radiation, hadronisation, colour reconnection, and cutoff values of the MPI mechanism, as well as the implementation of diffractive events. All MC models and tunes are able to predict the energy dependence on the charged-particle multiplicity as function of pseudorapidity, and give reasonable description for the different diffractive-enhanced event samples. A more complete discussion and comparison of MC event generators can be found in [1].

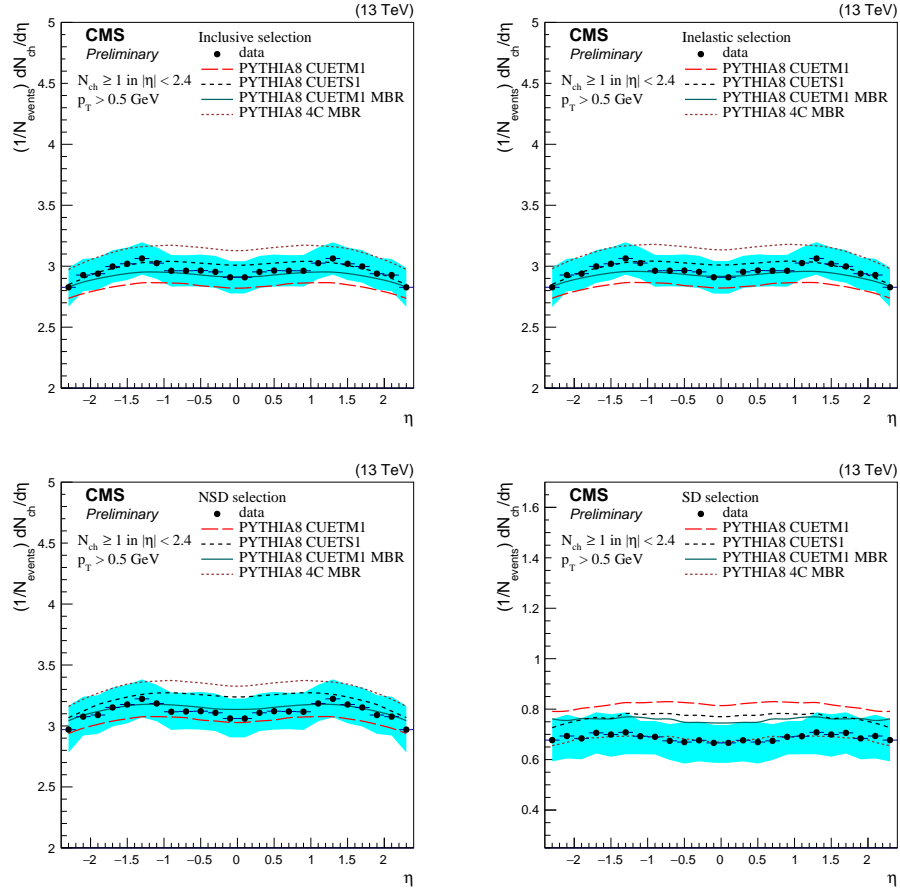


Figure 3: Charged-particle pseudorapidity density for the inclusive (top-left), inelastic-enhanced (top-right), NSD-enhanced (bottom-left) and SD-enhanced (bottom-right) event samples. The total systematic uncertainties are shown as shaded bands encompassing the data points.

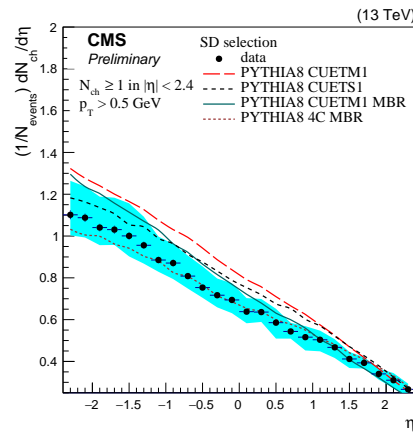


Figure 4: Charged-particle pseudorapidity density for the one-sided SD-enhanced event sample. The total systematic uncertainties are shown as shaded bands encompassing the data points.

References

- [1] CMS Collaboration, “Measurement of pseudorapidity distributions of charged particles in proton-proton collisions at $\sqrt{s} = 13$ TeV by the CMS experiment.”,
- [2] CMS Collaboration, “Pseudorapidity distribution of charged hadrons in proton-proton collisions at $\sqrt{s} = 13$ TeV”, *Phys. Lett. B* **751** (2015) 143–163, doi:[10.1016/j.physletb.2015.10.004](https://doi.org/10.1016/j.physletb.2015.10.004), arXiv:1507.05915.
- [3] J. Adam et al., “Pseudorapidity and transverse-momentum distributions of charged particles in proton-proton collisions at $\sqrt{s} = 13$ TeV”.
- [4] CMS Collaboration, “Measurement of pseudorapidity distributions of charged particles in proton-proton collisions at $\sqrt{s} = 8$ TeV by the CMS and TOTEM experiments”, *Eur. Phys. J. C* **74** (2014) 3053, doi:[10.1140/epjc/s10052-014-3053-6](https://doi.org/10.1140/epjc/s10052-014-3053-6).
- [5] CMS Collaboration, “Transverse momentum and pseudorapidity distributions of charged hadrons in pp collisions at $\sqrt{s} = 0.9$ and 2.36 TeV”, *JHEP* **02** (2010) 041, doi:[10.1007/JHEP02\(2010\)041](https://doi.org/10.1007/JHEP02(2010)041).
- [6] CMS Collaboration, “Transverse-momentum and pseudorapidity distributions of charged hadrons in pp collisions at $\sqrt{s} = 7$ TeV”, *Phys. Rev. Lett.* **105** (2010) 022002, doi:[10.1103/PhysRevLett.105.022002](https://doi.org/10.1103/PhysRevLett.105.022002).
- [7] ATLAS Collaboration, “Charged-particle multiplicities in pp interactions measured with the ATLAS detector at the LHC”, *New J. Phys.* **13** (2011) 053033, doi:[10.1088/1367-2630/13/5/053033](https://doi.org/10.1088/1367-2630/13/5/053033).
- [8] ALICE Collaboration, “Charged-particle multiplicity measurement in proton-proton collisions at $\sqrt{s} = 0.9$ and 2.36 TeV with ALICE at LHC”, *Eur. Phys. J. C* **68** (2010) 89, doi:[10.1140/epjc/s10052-010-1339-x](https://doi.org/10.1140/epjc/s10052-010-1339-x).
- [9] ALICE Collaboration, “Charged-particle multiplicity measurement in proton–proton collisions at $\sqrt{s} = 7$ TeV with ALICE at LHC”, *Eur. Phys. J. C* **68** (2010) 345, doi:[10.1140/epjc/s10052-010-1350-2](https://doi.org/10.1140/epjc/s10052-010-1350-2).
- [10] LHCb Collaboration, “Measurement of charged particle multiplicities in pp collisions at $\sqrt{s} = 7$ TeV in the forward region”, *Eur. Phys. J. C* **72** (2012) 1947, doi:[10.1140/epjc/s10052-012-1947-8](https://doi.org/10.1140/epjc/s10052-012-1947-8).
- [11] TOTEM Collaboration, “Measurement of the forward charged-particle pseudorapidity density in pp collisions at $\sqrt{s} = 7$ TeV with the TOTEM experiment”, *Europhys. Lett.* **98** (2012) 31002, doi:[10.1209/0295-5075/98/31002](https://doi.org/10.1209/0295-5075/98/31002).
- [12] CDF Collaboration, “Measurement of particle production and Inclusive Differential Cross Sections in $p\bar{p}$ Collisions at $\sqrt{s} = 1.96$ TeV”, *Phys. Rev. D* **79** (2009) 112005, doi:[10.1103/PhysRevD.79.112005](https://doi.org/10.1103/PhysRevD.79.112005). [Erratum doi:[10.1103/PhysRevD.82.119903](https://doi.org/10.1103/PhysRevD.82.119903)].
- [13] CDF Collaboration, “Pseudorapidity distributions of charged particles produced in $p\bar{p}$ interactions at $\sqrt{s} = 630$ GeV and 1800 GeV”, *Phys. Rev. D* **41** (1990) 2330, doi:[10.1103/PhysRevD.41.2330](https://doi.org/10.1103/PhysRevD.41.2330).
- [14] UA1 Collaboration, “A study of the general characteristics of proton-antiproton collisions at $\sqrt{s} = 0.2$ to 0.9 TeV”, *Nucl. Phys. B* **335** (1990) 261, doi:[10.1016/0550-3213\(90\)90493-W](https://doi.org/10.1016/0550-3213(90)90493-W).

- [15] UA4 Collaboration, “Pseudorapidity distribution of charged particles in diffraction dissociation events at the CERN SPS collider”, *Phys. Lett. B* **166** (1986) 459, [doi:10.1016/0370-2693\(86\)91598-4](https://doi.org/10.1016/0370-2693(86)91598-4).
- [16] UA5 Collaboration, “Scaling of pseudorapidity distributions at c.m. energies up to 0.9 TeV”, *Z. Phys. C* **33** (1986) 1, [doi:10.1007/BF01410446](https://doi.org/10.1007/BF01410446).
- [17] T. Sjöstrand, S. Mrenna, and P. Skands, “A brief introduction to PYTHIA 8.1”, *Comput. Phys. Commun.* **178** (2008) 852, [doi:10.1016/j.cpc.2008.01.036](https://doi.org/10.1016/j.cpc.2008.01.036).
- [18] P. Skands, S. Carrazza, and J. Rojo, “Tuning PYTHIA 8.1: the Monash 2013 Tune”, *Eur. Phys. J. C* **74** (2014), no. 8, 3024, [doi:10.1140/epjc/s10052-014-3024-y](https://doi.org/10.1140/epjc/s10052-014-3024-y), [arXiv:1404.5630](https://arxiv.org/abs/1404.5630).
- [19] CMS Collaboration, “Event generator tunes obtained from underlying event and multiparton scattering measurements”, *Eur. Phys. J. C* **76** (2016), no. 3, 155, [doi:10.1140/epjc/s10052-016-3988-x](https://doi.org/10.1140/epjc/s10052-016-3988-x), [arXiv:1512.00815](https://arxiv.org/abs/1512.00815).
- [20] R. Ciesielski and K. Goulianos, “MBR Monte Carlo Simulation in PYTHIA8”, *PoS ICHEP2012* (2013) 301, [arXiv:1205.1446](https://arxiv.org/abs/1205.1446).
- [21] R. Corke and T. Sjostrand, “Interleaved Parton Showers and Tuning Prospects”, *JHEP* **03** (2011) 032, [doi:10.1007/JHEP03\(2011\)032](https://doi.org/10.1007/JHEP03(2011)032), [arXiv:1011.1759](https://arxiv.org/abs/1011.1759).
- [22] M. Bähr et al., “Herwig++ physics and manual”, *Eur. Phys. J. C* **58** (2008) 639, [doi:10.1140/epjc/s10052-008-0798-9](https://doi.org/10.1140/epjc/s10052-008-0798-9), [arXiv:0803.0883](https://arxiv.org/abs/0803.0883).
- [23] M. H. Seymour and A. Siodmok, “Constraining MPI models using σ_{eff} and recent Tevatron and LHC Underlying Event data”, *JHEP* **10** (2013) 113, [doi:10.1007/JHEP10\(2013\)113](https://doi.org/10.1007/JHEP10(2013)113), [arXiv:1307.5015](https://arxiv.org/abs/1307.5015).
- [24] K. Werner, F. M. Liu, and T. Pierog, “Parton ladder splitting and the rapidity dependence of transverse momentum spectra in deuteron-gold collisions at RHIC”, *Phys. Rev. C* **74** (2006) 044902, [doi:10.1103/PhysRevC.74.044902](https://doi.org/10.1103/PhysRevC.74.044902), [arXiv:hep-ph/0506232](https://arxiv.org/abs/hep-ph/0506232).
- [25] T. Pierog et al., “EPOS LHC: test of collective hadronization with LHC data”, (2013), [arXiv:1306.0121](https://arxiv.org/abs/1306.0121).
- [26] T. Pierog, “LHC Results and High Energy Cosmic Ray Interaction Models”, *J. Phys.: Conf. Ser.* **409** (2013) 012008, [doi:10.1088/1742-6596/409/1/012008](https://doi.org/10.1088/1742-6596/409/1/012008).
- [27] CMS Collaboration, “Measurement of long-range near-side two-particle angular correlations in pp collisions at $\sqrt{s} = 13$ TeV”, [arXiv:1510.03068](https://arxiv.org/abs/1510.03068).
- [28] CMS Collaboration, “Description and performance of track and primary-vertex reconstruction with the CMS tracker”, *J. Instrum.* **9** (2014) P10009, [doi:10.1088/1748-0221/9/10/P10009](https://doi.org/10.1088/1748-0221/9/10/P10009).
- [29] CMS Collaboration, “Pseudorapidity distributions of charged particles in pp collisions at $\sqrt{s} = 7$ TeV with at least one central charged particle”, *CMS-PAS-QCD-10-024* (2011).